

École doctorale n° 364 : Sciences Fondamentales et Appliquées

## Doctorat ParisTech

### THÈSE

pour obtenir le grade de docteur délivré par

**L'École Nationale Supérieure des Mines de Paris**

**Spécialité doctorale “Science et Génie des Matériaux”**

*présentée et soutenue publiquement par*

**Ali SAAD**

le xx mai 2015

## NUMERICAL MODELLING OF MACROSEGREGATION INDUCED BY SOLIDIFICATION SHRINKAGE IN A LEVEL SET APPROACH

Directeurs de thèse: **Michel BELLET**  
**Charles-André GANDIN**

### Jury

<b>M. Blablabla</b> ,	Professeur, MINES ParisTech	Rapporteur
<b>M. Blablabla</b> ,	Professeur, Arts Et Métiers ParisTech	Rapporteur
<b>M. Blablabla</b> ,	Chargé de recherche, ENS Cachan	Examinateur
<b>M. Blablabla</b> ,	Danseuse, en freelance	Examinateur
<b>M. Blablabla</b> ,	Ingénieur, MIT	Examinateur

T  
H  
E  
S  
S



# Contents

<b>1 General Introduction</b>	<b>1</b>
1.1 Solidification notions . . . . .	2
1.1.1 Solute partitioning . . . . .	2
1.1.2 Dendritic growth . . . . .	4
1.1.3 Mush permeability . . . . .	6
1.2 Macrosegregation . . . . .	7
1.2.1 Liquid dynamics . . . . .	7
1.2.2 Solidification shrinkage . . . . .	8
1.2.3 Movement of equiaxed grains . . . . .	8
1.2.4 Solid deformation . . . . .	8
1.3 Other defects . . . . .	8
1.4 Industrial Worries . . . . .	10
1.5 Project context and objectives . . . . .	11
1.5.1 Context . . . . .	11
1.5.2 Objectives and outline . . . . .	12
<b>2 Modelling Review</b>	<b>15</b>
2.1 Modelling macrosegregation . . . . .	16
2.1.1 Macroscopic solidification model: monodomain . . . . .	17
2.2 Eulerian and Lagrangian motion description . . . . .	23
2.2.1 Overview . . . . .	23
2.2.2 Interface capturing . . . . .	25
2.3 Solidification models with level set . . . . .	25
2.4 The level set method . . . . .	26
2.4.1 Diffuse interface . . . . .	27
2.4.2 Mixing Laws . . . . .	28
2.5 Interface motion . . . . .	30
2.5.1 Level set transport . . . . .	31
2.5.2 Level set regularisation . . . . .	32

## Contents

---

<b>3 Energy balance with thermodynamic tabulations</b>	<b>37</b>
3.1 State of the art . . . . .	38
3.2 Thermodynamic considerations . . . . .	38
3.2.1 Volume averaging . . . . .	38
3.2.2 The temperature-enthalpy relationship . . . . .	39
3.2.3 Tabulation of properties . . . . .	40
3.3 Numerical method . . . . .	41
3.3.1 Enthalpy-based approach . . . . .	45
3.3.2 Temperature-based approach . . . . .	45
3.3.3 Convergence . . . . .	46
3.4 Validation . . . . .	47
3.4.1 Pure diffusion . . . . .	47
3.4.2 Convection and diffusion . . . . .	50
3.5 Application: multicomponent alloy solidification . . . . .	53
3.5.1 Tabulations . . . . .	55
3.5.2 Discussion . . . . .	56
<b>4 Macrosegregation with liquid metal motion</b>	<b>63</b>
4.1 Introduction . . . . .	64
4.2 Numerical treatment . . . . .	64
4.2.1 Stable mixed finite elements . . . . .	64
4.2.2 Variational multiscale (VMS) . . . . .	64
4.3 VMS solver . . . . .	65
4.4 Computational stability . . . . .	66
4.4.1 CFL condition . . . . .	66
4.4.2 Integration order . . . . .	66
4.5 Application to multicomponent alloys . . . . .	66
4.5.1 Results . . . . .	68
4.6 Macroscopic freckle prediction . . . . .	69
4.6.1 Introduction . . . . .	71
4.6.2 Experimental work . . . . .	72
4.6.3 Macroscopic scale simulations . . . . .	72
4.7 Meso-Macro freckle prediction . . . . .	79
4.7.1 Numerical method . . . . .	79
4.7.2 Configuration . . . . .	81
4.7.3 Effect of vertical temperature gradient . . . . .	84
4.7.4 Effect of cooling rate . . . . .	86
4.7.5 Effect of lateral temperature gradient . . . . .	88
4.7.6 Mono-grain freckles . . . . .	90

<b>5 Macrosegregation with solidification shrinkage</b>	<b>91</b>
5.1 Introduction . . . . .	92
5.2 FE model: Metal . . . . .	92
5.2.1 Mass and momentum conservation . . . . .	94
5.2.2 Energy conservation . . . . .	95
5.2.3 Species conservation . . . . .	97
5.3 FE model: Air . . . . .	99
5.3.1 Mass and momentum conservation . . . . .	100
5.3.2 Energy conservation . . . . .	100
5.3.3 Species conservation . . . . .	100
5.4 FE monolithic model . . . . .	100
5.4.1 Permeability mixing . . . . .	100
5.4.2 Model equations . . . . .	101
5.4.3 Interface treatment . . . . .	101
5.5 Shrinkage without macrosegregation . . . . .	103
5.5.1 Al-7wt% Si . . . . .	104
5.5.2 Pb-3wt% Sn . . . . .	104
5.6 Shrinkage with macrosegregation . . . . .	104
5.6.1 Al-7wt% Si . . . . .	104
5.6.2 Pb-3wt% Sn . . . . .	104
<b>Bibliography</b>	<b>105</b>

## **Contents**

---

---

<b>Acronym</b>	<b>Standing for</b>
ALE	Arbitrary Lagrangian-Eulerian
BTR	Brittleness temperature range
CCEMLCC	Chill Cooling for the Electro-Magnetic Levitator in relation with Continuous Casting of steel
CEMEF	Center for Material Forming
CSF	Continuum Surface Force
DLR	Deutsches Zentrum für Luft- und Raumfahrt
EML	Electromagnetic levitation
ESA	European Space Agency
FEM	Finite Element Method
GMAW	Gas Metal Arc Welding
ISS	International Space Station
IWT	Institut für Werkstofftechnik
LHS	Left Hand Side
LSM	Level set method
MAC	Marker-and-cell
MIN	Mini-element
PF	Phase field
RHS	Right Hand Side
RUB	Ruhr Universität Bochum
RVE	Representative Elementary Volume
SCPG	Shock Capturing Petrov-Galerkin
SUPG	Streamline Upwind Petrov-Galerkin
VMS	Variational MultiScale
VOF	Volume Of Fluid

---

## **Contents**

---

# Chapter 1

## General Introduction

Casting is one the earliest production techniques created by human civilisation since the Bronze Age, dated to circa 3000 BC. From ancient swords to nowadays toys, the need for alloys has never decreased. The key phenomenon behind this technique is solidification, or the transformation of matter from liquid to solid state. With this phase change, many phenomena, not visible to the naked eye, take place with a very complex interaction, in order to form a solid. However, the combination of thermal phenomena, like release of latent heat of solidification, and chemical phenomena like redistribution of chemical element atoms (also known as solute) with other atoms, often lead to *segregation*. The origins of this word from Latin, *segregatus*, has a social meaning of "separating a group from the dominant majority", while in metallurgy it means a non uniform distribution of chemical species. Depending on the scale, we may speak of *microsegregation* when the heterogeneity spans some few hundred microns, whereas the term *macrosegregation* refers to a much coarser length scale, ranging from some millimetres to some meters ! The final solid structure is has intrinsic thermophysical and thermomechanical properties directly influenced by the segregation pattern. In casting processes, such as continuous casting ([fig. 1.7](#)) and ingot casting, it is crucial to apprehend these intricate phenomena leading to macrosegregation as well as the influence on the final product, at each step of the process.

In this introductory chapter, we give a quick overview of solidification phenomena and microstructure, then present the factors which promote segregation, on both microscopic and macroscopic scales. Aside from macrosegregation, others defects are also briefly presented.

In a continuous casting process ([fig. 1.1a](#)), the partially solidified slab is carried through a series of rolls that exert contact forces to straighten it. As the mushy part of a slab enters through these rolls, interdendritic liquid is expelled backwards, i.e. in regions with lower solid fraction. Since the slab edges solidify earlier than the centre, the enriched liquid accumulates halfway in thickness, forming a centreline macrosegregation as shown in [fig. 1.2](#). Other types of segregates (channels, A-segregates ...) can also be

## Chapter 1. General Introduction

---

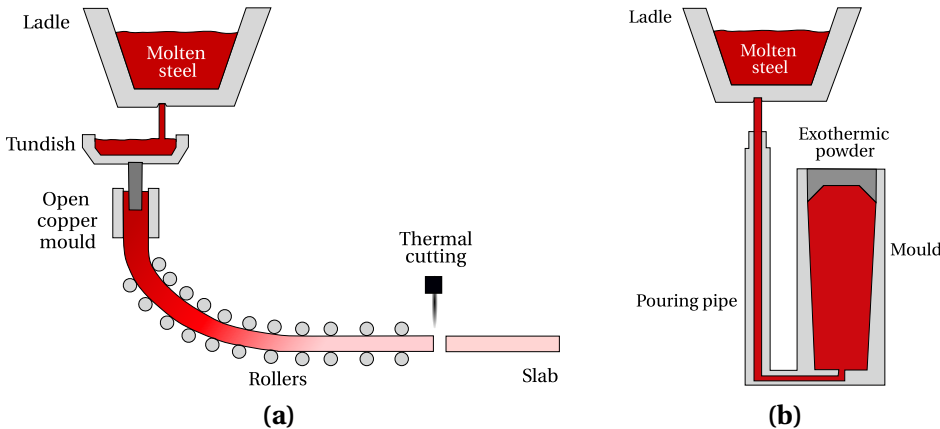


**Fig. 1.1 – Main processes for steelmaking by (a) continuous casting or (b) ingot casting**

found but remain more specific to ingot casting. A variety of segregation patterns can be encountered while casting heavy ingots, as in [fig. 1.1b](#):

- the lower part is characterized by a negative segregation cone promoted by the sedimentation of equiaxed crystals and settling of dendrite fragments,
- positive segregation channels, known as A-segregates, form along the columnar dendritic zones, close to the vertical contact with the mould,
- positive V-segregates can be identified in the centre of the ingot,
- a positive "hot-top" macrosegregation in the upper zone where the last rich liquid solidifies, caused by solidification shrinkage and thermosolutal buoyancy forces.

[Combeau et al. \[2009\]](#) state that A-segregates and V-segregates formation is mainly attributed to local flow phenomena. As such, their scale is finer than macrosegregation, hence called "mesosegregates".

## 1.1 Solidification notions

### 1.1.1 Solute partitioning

The simplest definition is of this phenomenon is an uneven distribution of solute between the liquid and the growing solid, at the microscopic scale of the interface separating these phases. If we consider a binary alloy, then the solubility limit is the key factor that dictates the composition at which a primary solid phase exists at equilibrium. The segregation (or partition) coefficient  $k$  determines the extent of solute rejection into the liquid during solidification:

$$k = \frac{w^{s^*}}{w^{l^*}} \quad (1.1)$$

## 1.1. Solidification notions

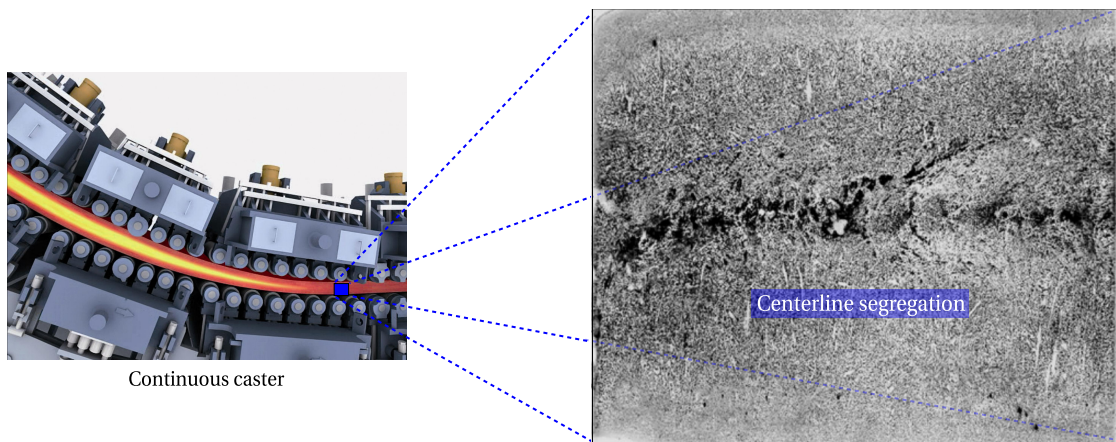


**Fig. 1.2** – Zoom on a sulphur print of a continuously cast high carbon steel billet at a longitudinal section, showing high positive centreline segregation [Choudhary et al. 1994].

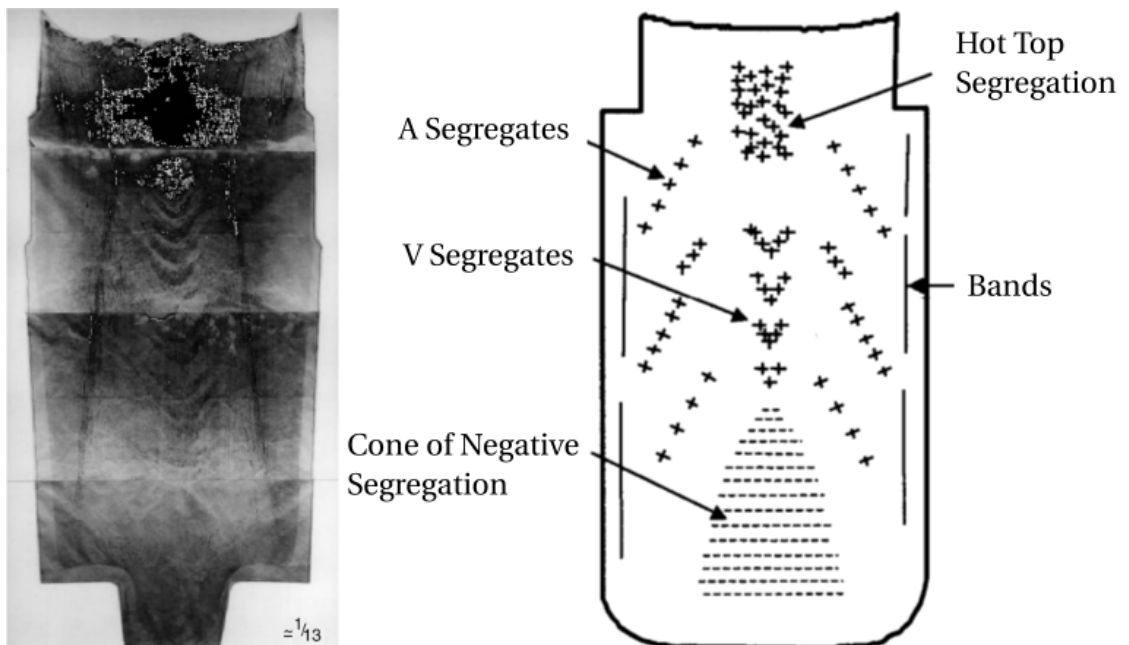


**Fig. 1.3** – Sulphur print (left) of a 65-ton steel ingot [Lesoult 2005] showing various patterns (right) of macrosegregation [Flemings 1974]

## Chapter 1. General Introduction

---

where  $w^{s*}$  and  $w^{l*}$  are the compositions of the solid and liquid respectively, at the interface. When the segregation coefficient is less than unity (such is the case for most alloys during dendritic solidification), the first solid forms at the liquidus temperature,  $T$ , with a composition  $w^{s*} = kw^{l*} = kw_0$  less than the liquid's composition  $w_0$ , the latter being initially at the nominal composition,  $w_0$ . [Figure 1.4](#) illustrates a typical binary phase diagram where the real solidus and liquidus are represented by solid lines, while the possible linear approximations are in grey dashed lines. For most binary alloys, this linearisation simplifies derivation of microsegregation models, as  $k$  becomes independent of temperature.

For each phase, the relationship between the composition at the interface and that in the bulk depends on the chemical homogenisation (i.e. solute diffusivity) of the phase. The more homogeneous a phase, the closer the concentrations between the interface and the bulk, hence closer to equilibrium. It is thus essential to study the effect of homogenisation on the segregation behaviour and the subsequent effect on solidification, which is seen by a non-uniform composition through the cast product on a microscopic scale, better known as microsegregation. This phenomenon is essential in a casting process inasmuch as it affects the microstructure and grain morphology, hence the final mechanical properties of the alloy.

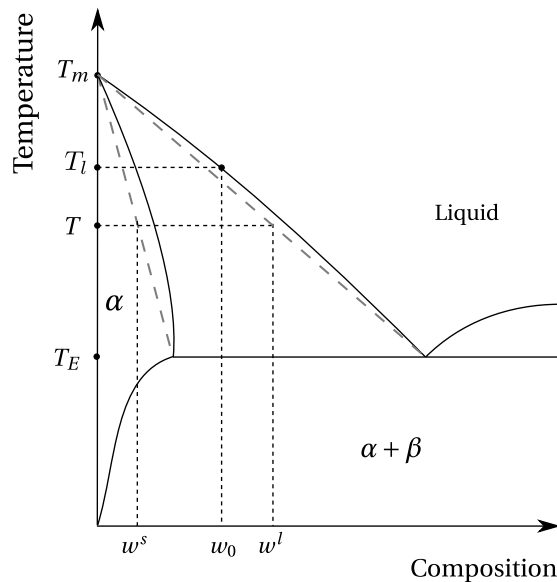


**Fig. 1.4** – Typical eutectic phase diagram of a binary alloy showing the real solidus and liquidus at full equilibrium, with the corresponding linear approximations (grey dashed lines).  $T_m$  and  $T_E$  are respectively the melting point of the solvent and the eutectic temperature.

### 1.1.2 Dendritic growth

In a casting process, the chill surface i.e. the contact between the molten alloy and relatively cold moulds, is the first area to solidify. Thermal gradient,  $G$ , and cooling rate,

$R$ , are two crucial process parameters that define the solid-liquid interface velocity,  $v^*$ , which in turn affects the initial microstructure. Although it may be not easy to control them, their crucial role in solidification is well established.

The solid-liquid interface fluctuates when solidifying, thus perturbations may appear on the front, locally destabilizing it. Two outcome scenarios are possible. The first sce-

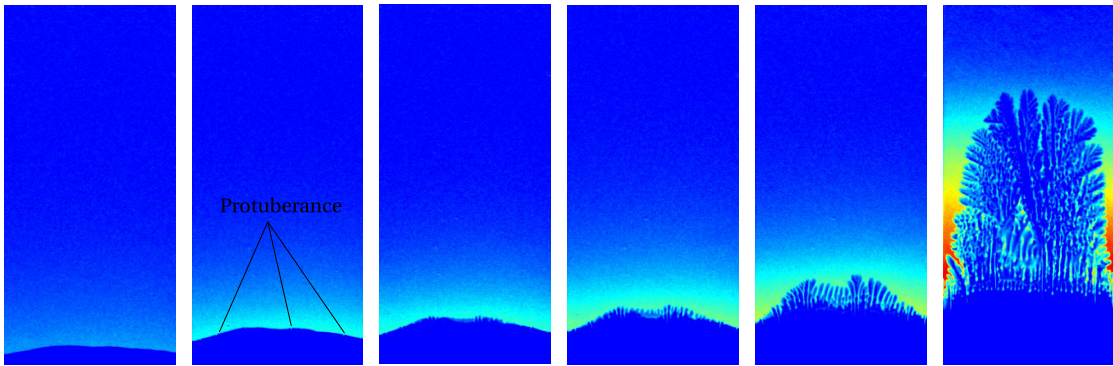


**Fig. 1.5** – Time evolution of a solidifying Al-4 wt.% Cu sample, showing interface destabilisation and subsequent dendritic solidification [Buffet et al. 2010]. The liquid far from the interface and having a blue color is at nominal composition, while the one near the dendritic structure with the yellow and red colors, is richer in solute.

nario is characterized by low values of  $v^*$  where the interface maintains a planar shape, hence we speak of *planar growth*. With this kind of growth, a random protuberance appearing at the interface, has a low tip velocity (low driving force of solidification). As such, the rest of the interface catches up, maintaining the planar geometry. In another scenario more representative of a real casting, the interface speed is greater in general, due to high solidification rate. The protuberance tip will be pulled into a liquid less rich in solute than the interface, as shown in the time frames of fig. 1.5. The zone ahead of the solid-liquid interface is constitutionally undercooled [Tiller et al. 1953], giving a greater driving force for the protuberance to grow in the direction of the thermal gradient. As the solid-liquid interface adopts a tree-like shape, we speak of *dendritic growth*. Near the chill surface, dendrites are columnar, with a favourable growth in the  $\langle 100 \rangle$  direction for alloys with cubic lattices, but different orientations are also reported in the literature [see Dantzig et al. 2009, p. 289]. Far from mould walls, a similar dendritic growth phenomenon occurs where temperature is uniform, but with an equiaxed morphology. ?? shows both columnar and equiaxed morphologies. Columnar dendrites are characterized by a primary spacing,  $\lambda_1$ , between the main trunks, and a secondary spacing,  $\lambda_2$ , for the arms that are perpendicular to the trunks. It should be noted that  $\lambda_1$  and  $\lambda_2$ , together with the grain size, are three important microstructural parameters in the as-cast microstructure [Easton et al. 2011]. Further branching may occur but will not be discussed here.

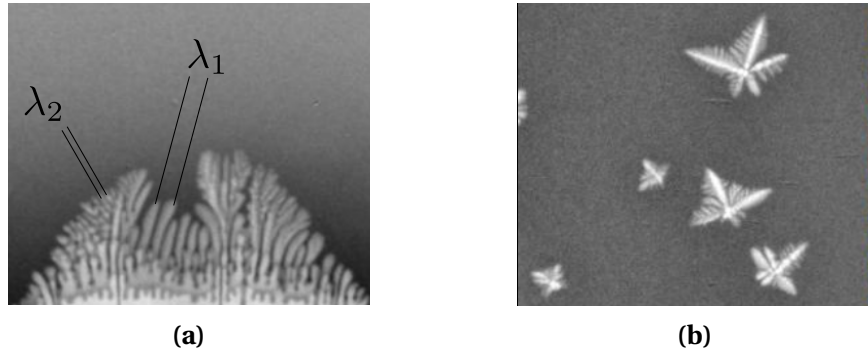


**Fig. 1.6** – In situ observation by X-ray radiography of the (a) columnar microstructure for Al-4 wt.% Cu alloy [Buffet et al. 2010] and (b) equiaxed microstructure during solidification of Al-10 wt.% Cu alloy [Bogno et al. 2013].

### 1.1.3 Mush permeability

The dendritic geometry is crucial in solidification theory as it exhibits lower solid fraction compared to a microstructure formed by planar growth. This fact has consequences on the fluid-structure interaction in the mushy zone, namely the liquid flow through dendrites. At the chill surface, the solid grows gradually from dispersed growing nuclei to a permeable solid skeleton, until finally grains have fully grown at the end of phase change. In the intermediate state, the liquid flow in and out of the mushy zone through the dendrites is a key phenomenon from a rheological perspective. The flow through the solid skeleton is damped by primary and secondary dendrites, resulting in momentum dissipation just like in saturated porous media. The famous Darcy [1856] law relates the pressure gradient ( $\vec{\nabla}p$ ) to the fluid velocity  $\vec{v}$  (assuming a the solid phase is fixed), through the following equation [Rappaz et al. 2003]:

$$\vec{v} = \frac{\mathbb{K}}{\mu^l} \vec{\nabla}p \quad (1.2)$$

where  $\mu^l$  is the liquid dynamic viscosity and  $\mathbb{K}$  is the permeability tensor. The latter parameter has been the subject of numerous studies that aimed to predict it from various microstructural or morphological parameters. Some of these studies have started even before the first attempts to model macrosegregation by Flemings et al. [1967], Flemings et al. [1968a], and Flemings et al. [1968b]. Basically, all models include the solid fraction,  $g^s$ , as input to predict mush permeability along with empirical data. An instance of such models is the work of Xu et al. [1991]. Some models rely additionally on the primary dendrite arm spacing  $\lambda_1$  like Blake-Kozeny [Ramirez et al. 2003], or the secondary dendrite arm spacing  $\lambda_2$  like Carman-Kozeny, as a meaningful parameter to determine an isotropic permeability. Other models like Poirier [1987] and Felicelli et al. [1991] derive an anisotropic permeability based on both  $\lambda_1$  and  $\lambda_2$ .

The present work uses Carman-Kozeny as a constitutive model for the isotropic per-

meability scalar (zero order tensor):

$$\mathbb{K} = \frac{\lambda_2^2 g^{l^3}}{180 (1 - g^l)^2} \quad (1.3)$$

## 1.2 Macrosegregation

Macrosegregation generally stems from a solubility difference between a liquid phase and one or more solid phases, along with a relative velocity between these phases. While the former is responsible for local solute enrichment or depletion, the latter will propagate the composition heterogeneity on a scale much larger than just a few dendrites. This is why macrosegregation could be observed on the scale of a casting, up to several meters in length. While microsegregation can be healed by annealing the alloy to speed up the diffusion process and allow homogenization, heterogeneities spanning on larger distances cannot be treated after solidification. It is obvious that macrosegregation is irreversible defect. Failure to prevent it, may lead to a substantial decline in the alloy's mechanical behaviour, hence its serviceability. Four main factors can (simultaneously) cause fluid flow leading to macrosegregation:

### 1.2.1 Liquid dynamics

During solidification, thermal and solutal gradients result in density gradients in the liquid phase:

$$\rho^l = \rho_0^l (1 - \beta_T (T - T_0) - \sum_i \beta_{w_i^l} (w_i^l - \langle w_i \rangle_0^l)) \quad (1.4a)$$

$$\vec{\nabla} \rho^l = -\rho_0^l (\beta_T \vec{\nabla} T + \sum_i \beta_{w_i^l} \vec{\nabla} w_i^l) \quad (1.4b)$$

In eq. (1.4a), density is assumed to vary linearly with temperature and phase composition for each chemical species (index  $i$ ). The slopes defining such variations are respectively the thermal expansion coefficient  $\beta_T$  and the solutal expansion coefficients  $\beta_{w_i^l}$ , given by:

$$\beta_T = -\frac{1}{\rho_0^l} \left( \frac{\partial \rho^l}{\partial T} \right) \quad (1.5a)$$

$$\beta_{w_i^l} = -\frac{1}{\rho_0^l} \left( \frac{\partial \rho^l}{\partial w_i^l} \right) \quad (1.5b)$$

The linear fit assumes also that the density takes a reference value,  $\rho_0^l$ , when temperature and liquid composition reach reference values, respectively  $T_0$  and  $\langle w_i \rangle_0^l$ , while the coefficients  $\beta_{w_i^l}$  remain constant. However, in some situations, a suitable ther-

## Chapter 1. General Introduction

---

modynamic database providing accurate density values is far better than a linear fit, especially in the current context of macrosegregation. In the presence of gravity, the density gradient in eq. (1.4b), causes thermosolutal convection in the liquid bulk and a subsequent macrosegregation.

### 1.2.2 Solidification shrinkage

Solid alloys generally have a greater density than the liquid phase ( $\rho^s > \rho^l$ ), thus occupy less volume, with the exception of silicon where the opposite is true. Upon solidification, the liquid moves towards the solidification front to compensate for the volume difference caused by the phase change, as well as the thermal contraction. When macrosegregation is triggered by solidification shrinkage, we speak of *inverse segregation*: while one would naturally expect negative macrosegregation in areas where solidification begins and positive inside the alloy, shrinkage promotes the opposite phenomenon, by bringing solute-richer liquid towards the solidifying areas, thus raising their solute content, and resulting in a positively segregated solid. In contrast to liquid convection, shrinkage flow may cause macrosegregation even without gravity.

### 1.2.3 Movement of equiaxed grains

Equiaxed grains can grow in the liquid bulk where thermal gradients are weak, or in the presence of inoculants. Consequently, they are transported by the flow (floating or sedimenting, depending on their density [Beckermann 2002]) which leads to negative macrosegregation in their final position.

### 1.2.4 Solid deformation

Stresses of thermal and mechanical nature are always found in casting processes (e.g. bulging between rolls in continuous casting). Deformation of the semi-solid in the mushy zone causes a relative solid-liquid flow in the inward (tensile stresses) or outward (compressive stresses) direction, causing macrosegregation.

## 1.3 Other defects

Defects are encountered in any industrial process. More importantly, a lot of them in the casting industry can be disastrous when the cast product is unserviceable and rejected. This leads to a systematic product recycling, i.e. the product is ditched to be reheated (if possible), remelted and then cast again. From an economic point view, the operation is very expensive. Understanding and preventing defects when possible

is thus crucial in the casting industry. We briefly list hereafter the main encountered defects.

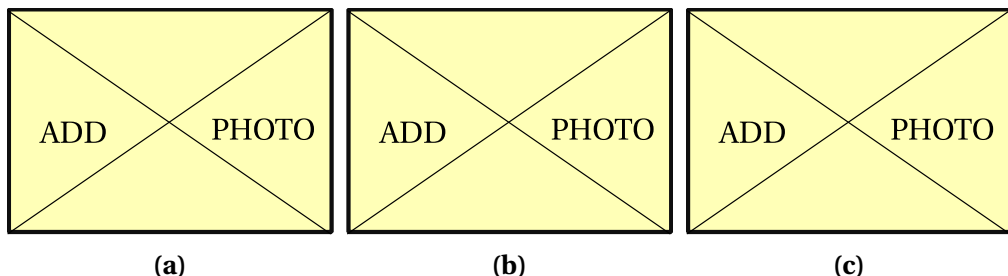


**Fig. 1.7** – Three instances of solidification-related defects found in cast products: (a) asdads (b) df sdf and (c) fd sf sf.

### Hot tearing

This defect, also denoted solidification cracking or hot cracking, occurs in the mushy zone at high solid fractions when a failure or crack appears at specific locations, the hot spots. The temperature range in which the steel is vulnerable to hot tearing is known as the brittleness temperature range (BTR). It corresponds to solid fractions greater than 90%, where the liquid phase starts to form a discontinuous film. Many factors can initiate the failure, but the main origin is a lack of liquid feeding required to compensate for the solidification shrinkage, in the presence of thermal stresses in the mushy region. Therefore, a crack initiates and then propagates in the casting.

### Porosity

Porosity is a void defect formed inside the casting or at the outer surface. It may be attributed to two different factors. Firstly, we speak of *shrinkage porosity*, when a void forms as a result of density differences between the liquid and its surrounding dendritic solid network, the latter being generally denser than the former. The second factor is the presence of dissolved gaseous phases in the melt. According to Dantzig et al. [2009], these gases may be initially in the melt, or created by the reaction between the metal and water found in the air or trapped in grooves at the moulds surface. Providing sufficient cooling and pressure drop in the liquid, the latter becomes supersaturated. The nucleation of a gaseous phase is then triggered.

### Freckles or segregated channels

The origin of this defect is a combined effect of microsegregation and buoyancy forces. Upon solidification, solid forms while exchanging solutes with the liquid due to partitioning. For a solute species that preferentially segregates into the liquid (partition

coefficient less than unity) and locally reduce the liquid density, a solutal driving force is created inside the mushy zone, generating convection currents, with "plume" shapes as often reported in the literature [Sarazin et al. 1992; Schneider et al. 1997; Shevchenko et al. 2013]. Temperature gradient is often an additional force of convection as the liquid densoty depends also temperature-dependent, the resulting driving force is then qualified as "thermosolutal".

## 1.4 Industrial Worries

**Steel production** has continuously increased over the years to meet the industrial needs. [Figure 1.8](#) shows this increase between 1980 and 2013 with a clear dominance of the Chinese production. Quality constraints have also increased where specific grades of steel are needed in critical applications such as mega-structures in construction and heavy machinery. Therefore, alloys with defects are considered vulnerable and should be avoided as much as possible during the casting process. As such, steelmakers have been investing in research, with the aim of understanding better the phenomena leading to casting problems, and improve the processes when possible.

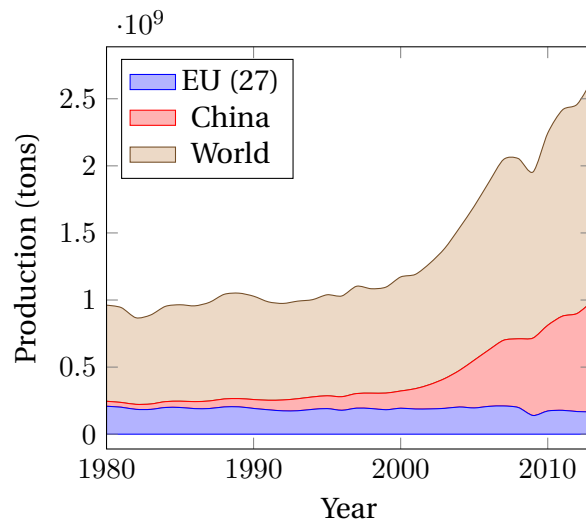


**Fig. 1.8** – Evolution curves of crude steel worldwide production from 1980 to 2013 [[WSA 2014](#)].

**Simulation software** dedicated to alloy casting is one of the main research investments undertaken by steelmakers. These tools coming from academic research are actively used to optimize the process. However, few are the tools that take into account the casting environment. For instance, the continuous casting process, in [fig. 1.7](#), is a chain process where the last steps involve rolls, water sprays and other components. A dedicated software is one that can provide the geometric requirements with suitable meshing capabilities, as well as respond to metallurgical and mechanical requirements, mainly by handling:

- moulds and their interaction with the alloy (thermal resistances ...)
- alloy filling and predicting velocity in the liquid and mushy zone
- thermomechanical stresses in the solid
- multicomponent alloys and predicting macrosegregation
- microstructure and phases
- finite solute diffusion in solid phases
- real alloy properties (not just constant thermophysical/thermomechanical properties)

## **1.5 Project context and objectives**

### **1.5.1 Context**

The European Space Agency (ESA) has been actively committed, since its foundation in 1975, in the research field. Its covers not only exclusive space applications, but also fundamental science like solidification. This thesis takes part in the ESA project entitled *CCEMLCC*, abbreviating "Chill Cooling for the Electro-Magnetic Levitator in relation with Continuous Casting of steel". The three-year contract from 2011 to late 2014 denoted *CCEMLCC II*, was preceded by an initial project phase, *CCEMLCC I*, from 2007 to 2009. The main focus is studying containerless solidification of steel under microgravity conditions. A chill plate is used to extract heat from the alloy, simulating the contact effect with a mould in continuous casting or ingot casting. A partnership of 7 industrial and academic entities was formed in *CCEMLCC II*. Here is a brief summary of each partner's commitment:

#### **Academic partners**

- Center for Material Forming (CEMEF) - France: numerical modelling of microgravity chill cooling experiments
- Deutsches Zentrum für Luft- und Raumfahrt (DLR or German Aerospace Centre) and Ruhr Universität Bochum (RUB) university - Germany: preparation of a chill cooling device for electromagnetic levitation (EML), microgravity testing and investigation of growth kinetics in chill-cooled and undercooled steel alloys
- University of Alberta - Canada: impulse atomization and spray deposition of the D2 tool steel
- University of Bremen - Institut für Werkstofftechnik (IWT) institute - Germany: study of D2 tool steel melt solidification in atomization processing

#### **Industrial partners**

## Chapter 1. General Introduction

---

- ARCELORMITTAL (France): elaboration of a series of steel grades used in microgravity and ground-based studies
- METSO Minerals Inc. (Finland): material production with D2 tool steel for spray forming
- TRANSVALOR (France): development and marketing of the casting simulation software *Thercast<sup>®</sup>*

CEMEF, as an academic partner, contributed to the work by proposing numerical models in view of predicting the chill cooling of steel droplets. A first model was developed by Rivaux [2011]. The experimental work by DLR considered various facilities and environments to set a droplet of molten alloy in levitation: EML (fig. 1.9) for ground-based experiments, microgravity during parabolic flight or sounding rockets and last, microgravity condition on-board the International Space Station (ISS).



**Fig. 1.9 – Electromagnetic levitation [DLR 2014].**

### 1.5.2 Objectives and outline

The main focus of the present thesis is predicting macrosegregation with liquid dynamics assuming a fixed solid phase, i.e. no account of solid transport (e.g. equiaxed crystals sedimentation) and no account of solid deformation. At CEMEF, this scope has been adopted in previous studies by Gouttebroze [2005], Liu [2005], Mosbah [2008], Rivaux [2011], and Carozzani [2012]. Nevertheless, many modelling features evolved with time such as going from two-dimensional to three-dimensional modelling, resolution schemes for each of the conservation equations: energy, chemical species and liquid momentum, Eulerian or Lagrangian descriptions, modelling of grain structure and others. In this thesis, we propose a numerical model that takes into account i) the energy conservation in a temperature formulation based on a thermodynamic database mapping, ii) the liquid momentum conservation with thermosolutal convection and solidification shrinkage as driving forces, iii) solute mass conservation with solidification shrinkage (to predict inverse segregation) and iv) solidification paths at full equilibrium for multicomponent alloys. Moreover, all equations are formulated in a pure Eulerian description while using the Level Set method to keep implicitly track of the interface between the alloy and the surrounding gas. To the author's knowledge,

## 1.5. Project context and objectives

---

this work combining macrosegregation prediction using the level set methodology to track the metal-air interface during shrinkage has no precedent in casting and solidification literature. The model couples in a weak fashion, all four conservation equations presented in [fig. 1.10](#), showing on the one hand, that microsegregation is an essential common link between these equations, while on the other hand, the level set interacts with conservations equations by giving the interface position.

Numerical tools: Cimlib relying on PETSc, parallelised with MPICH2, paraview and python as tools for postprocess and analysis.

The previously mentionned simulation requirements are not met in a single casting software package. Nevertheless, *Thercast®* is a promising tool that already handles a part of the above points. The current thesis developments are done using C++ language as a part of the in-house code, known as *CimLib* [[Digonnet et al. 2007](#); [Mesri et al. 2009](#)]. This fully parallel library is the main academic research support for *Thercast®*

Outline: each chapter content ...

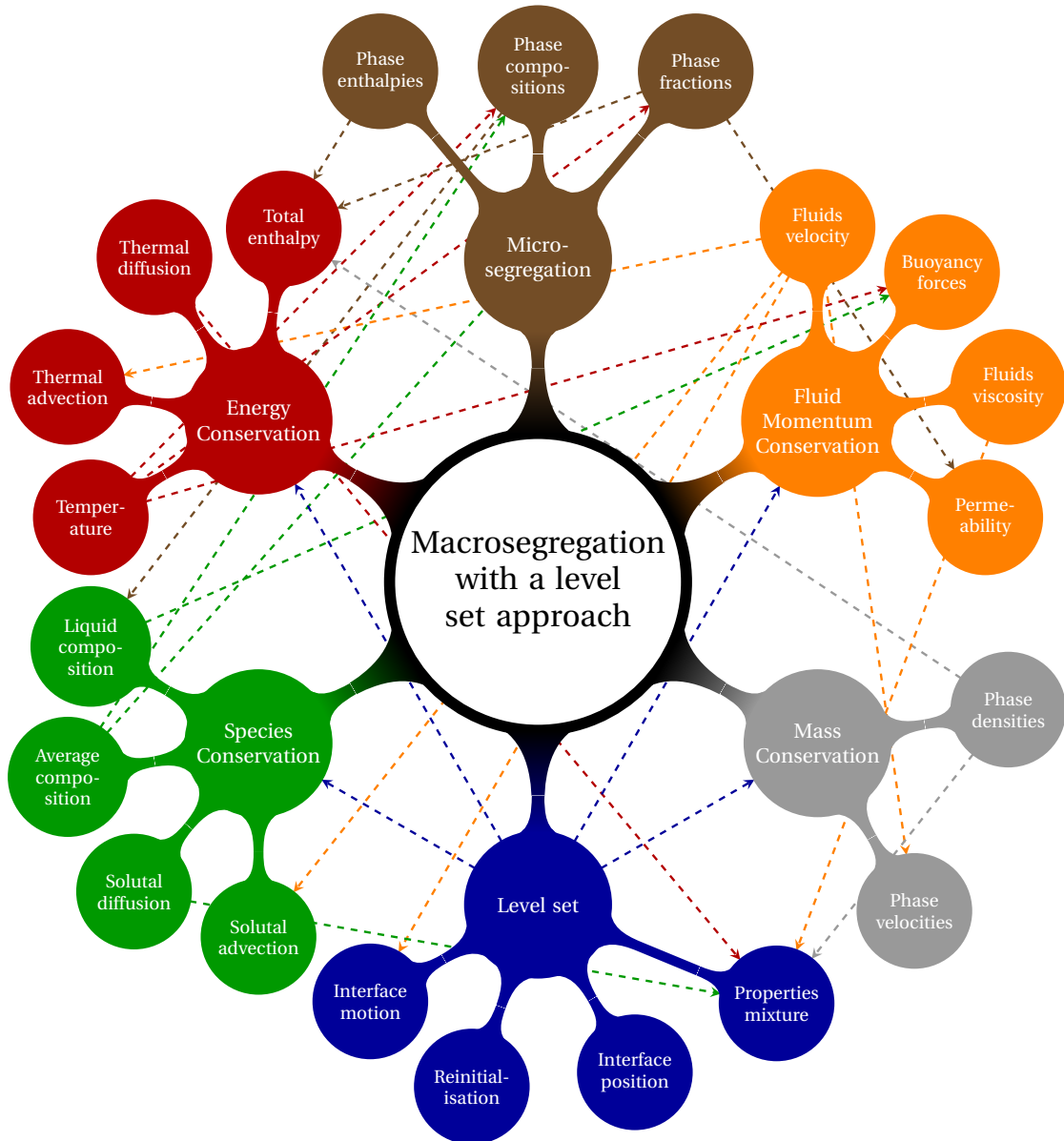


**Fig. 1.10** – A graphical representation of the main ingredients of the numerical approach, for a macrosegregation model with the level set methodology, when no solid deformation or movement are considered. The dashed lines represent the possible interaction between the components.

# Bibliography

## [Beckermann 2002]

Beckermann, C. (2002). "Modelling of macrosegregation: applications and future needs". *International Materials Reviews*, 47 (5), pp. 243–261. URL: <http://www.maneyonline.com/doi/abs/10.1179/095066002225006557> (cited on page 8).

## [Bogno et al. 2013]

Bogno, A., Nguyen-Thi, H., Reinhart, G., Billia, B., and Baruchel, J. (2013). "Growth and interaction of dendritic equiaxed grains: In situ characterization by synchrotron X-ray radiography". *Acta Materialia*, 61 (4), pp. 1303–1315. URL: <http://www.sciencedirect.com/science/article/pii/S1359645412008026> (cited on page 6).

## [Buffet et al. 2010]

Buffet, A. et al. (2010). "Measurement of Solute Profiles by Means of Synchrotron X-Ray Radiography during Directional Solidification of Al-4 wt% Cu Alloys". *Materials Science Forum*, 649, pp. 331–336. URL: <http://www.scientific.net/MSF.649.331> (cited on pages 5, 6).

## [Carozzani 2012]

Carozzani, T. (2012). "Développement d'un modèle 3D Automate Cellulaire-Éléments Finis (CAFE) parallèle pour la prédiction de structures de grains lors de la solidification d'alliages métalliques". PhD Thesis. Ecole Nationale Supérieure des Mines de Paris. URL: <http://pastel.archives-ouvertes.fr/pastel-00803282> (cited on page 12).

## [Choudhary et al. 1994]

Choudhary, S. K. and Ghosh, A. (1994). "Morphology and Macrosegregation in Continuously Cast Steel Billets." *ISIJ International*, 34 (4), pp. 338–345. URL: <http://ci.nii.ac.jp/naid/130000781622> (cited on page 3).

## [Combeau et al. 2009]

Combeau, H., Založník, M., Hans, S., and Richy, P. E. (2009). "Prediction of Macrosegregation in Steel Ingots: Influence of the Motion and the Morphology of Equiaxed Grains". *Metallurgical and Materials Transactions B*, 40 (3), pp. 289–304. URL: <http://link.springer.com/article/10.1007/s11663-008-9178-y> (cited on page 2).

## [Dantzig et al. 2009]

Dantzig, J. A. and Rappaz, M. (2009). *Solidification*. EPFL Press (cited on pages 5, 9).

## Bibliography

---

### [Darcy 1856]

Darcy, H. (1856). *Les fontaines publiques de la ville de Dijon : exposition et application des principes à suivre et des formules à employer dans les questions de distribution d'eau*. V. Dalmont (Paris). URL: <http://gallica.bnf.fr/ark:/12148/bpt6k624312> (cited on page 6).

### [Digonnet et al. 2007]

Digonnet, H., Silva, L., and Coupez, T. (2007). "Cimlib: A Fully Parallel Application For Numerical Simulations Based On Components Assembly". *AIP Conference Proceedings*. Vol. 908. AIP Publishing, pp. 269–274. URL: <http://scitation.aip.org/content/aip/proceeding/aipcp/10.1063/1.2740823> (cited on page 13).

### [DLR 2014]

DLR (2014). *ElectroMagnetic Levitation*. <http://goo.gl/e5JhiA> (cited on page 12).

### [Easton et al. 2011]

Easton, M., Davidson, C., and StJohn, D. (2011). "Grain Morphology of As-Cast Wrought Aluminium Alloys". *Materials Transactions*, 52 (5), pp. 842–847 (cited on page 5).

### [Felicelli et al. 1991]

Felicelli, S. D., Heinrich, J. C., and Poirier, D. R. (1991). "Simulation of freckles during vertical solidification of binary alloys". *Metallurgical Transactions B*, 22 (6), pp. 847–859. URL: <http://link.springer.com/article/10.1007/BF02651162> (cited on page 6).

### [Flemings 1974]

Flemings, M. C. (1974). "Solidification processing". *Metallurgical Transactions*, 5 (10), pp. 2121–2134. URL: <http://link.springer.com/article/10.1007/BF02643923> (cited on page 3).

### [Flemings et al. 1967]

Flemings, M. C. and Nereo, G. E. (1967). "Macrosegregation: Part I". *Transactions of the Metallurgical Society of AIME*, 239, pp. 1449–1461 (cited on page 6).

### [Flemings et al. 1968a]

Flemings, M. C., Mehrabian, R., and Nereo, G. E. (1968a). "Macrosegregation: Part II". *Transactions of the Metallurgical Society of AIME*, 242, pp. 41–49 (cited on page 6).

### [Flemings et al. 1968b]

Flemings, M. C. and Nereo, G. E. (1968b). "Macrosegregation: Part III". *Transactions of the Metallurgical Society of AIME*, 242, pp. 50–55 (cited on page 6).

### [Gouttebroze 2005]

Gouttebroze, S. (2005). "Modélisation 3d par éléments finis de la macroségrégation lors de la solidification d'alliages binaires". PhD thesis. École Nationale Supérieure des Mines de Paris. URL: <https://pastel.archives-ouvertes.fr/pastel-00001885/document> (cited on page 12).

**[Lesoult 2005]**

Lesoult, G. (2005). "Macrosegregation in steel strands and ingots: Characterisation, formation and consequences". *Materials Science and Engineering: A, International Conference on Advances in Solidification Processes* 413–414, pp. 19–29. URL: <http://www.sciencedirect.com/science/article/pii/S0921509305010063> (cited on page 3).

**[Liu 2005]**

Liu, W. (2005). "Finite Element Modelling of Macrosegregation and Thermomechanical Phenomena in Solidification Processes". PhD thesis. École Nationale Supérieure des Mines de Paris. URL: <http://pastel.archives-ouvertes.fr/pastel-00001339> (cited on page 12).

**[Mesri et al. 2009]**

Mesri, Y., Digonnet, H., and Coupez, T. (2009). "Advanced parallel computing in material forming with CIMLib". *European Journal of Computational Mechanics/Revue Européenne de Mécanique Numérique*, 18 (7-8), pp. 669–694. URL: <http://www.tandfonline.com/doi/abs/10.3166/ejcm.18.669-694> (cited on page 13).

**[Mosbah 2008]**

Mosbah, S. (2008). "Multiple scales modeling of solidification grain structures and segregation in metallic alloys". PhD thesis. École Nationale Supérieure des Mines de Paris. URL: <https://tel.archives-ouvertes.fr/tel-00349885/document> (cited on page 12).

**[Poirier 1987]**

Poirier, D. R. (1987). "Permeability for flow of interdendritic liquid in columnar-dendritic alloys". *Metallurgical Transactions B*, 18 (1), pp. 245–255. URL: <http://link.springer.com/article/10.1007/BF02658450> (cited on page 6).

**[Ramirez et al. 2003]**

Ramirez, J. C. and Beckermann, C. (2003). "Evaluation of a rayleigh-number-based freckle criterion for Pb-Sn alloys and Ni-base superalloys". *Metallurgical and Materials Transactions A*, 34 (7), pp. 1525–1536. URL: <http://link.springer.com/article/10.1007/s11661-003-0264-0> (cited on page 6).

**[Rappaz et al. 2003]**

Rappaz, M., Bellet, M., and Deville, M. (2003). *Numerical Modeling in Materials Science and Engineering*. Springer Series in Computational Mathematics. Springer Berlin Heidelberg (cited on page 6).

**[Rivaux 2011]**

Rivaux, B. (2011). "Simulation 3D éléments finis des macroségrégations en peau induites par déformations thermomécaniques lors de la solidification d'alliages métalliques". PhD Thesis. École Nationale Supérieure des Mines de Paris. URL: <http://pastel.archives-ouvertes.fr/pastel-00637168> (cited on page 12).

**[Sarazin et al. 1992]**

Sarazin, J. R. and Hellawell, A. (1992). "Studies of Channel-Plume Convection during Solidification". *Interactive Dynamics of Convection and Solidification*. Ed. by S. H. Davis,

## Bibliography

---

H. E. Huppert, U. Müller, and M. G. Worster. NATO ASI Series 219. Springer Netherlands, pp. 143–145. URL: [http://link.springer.com/chapter/10.1007/978-94-011-2809-4\\_22](http://link.springer.com/chapter/10.1007/978-94-011-2809-4_22) (cited on page 10).

### [Schneider et al. 1997]

Schneider, M. C., Gu, J. P., Beckermann, C., Boettigner, W. J., and Kattner, U. R. (1997). “Modeling of micro- and macrosegregation and freckle formation in single-crystal nickel-base superalloy directional solidification”. *Metallurgical and Materials Transactions A*, 28 (7), pp. 1517–1531. URL: <http://link.springer.com/article/10.1007/s11661-997-0214-3> (cited on page 10).

### [Shevchenko et al. 2013]

Shevchenko, N., Boden, S., Gerbeth, G., and Eckert, S. (2013). “Chimney Formation in Solidifying Ga-25wt pct In Alloys Under the Influence of Thermosolutal Melt Convection”. *Metallurgical and Materials Transactions A*, 44 (8), pp. 3797–3808. URL: <http://link.springer.com/article/10.1007/s11661-013-1711-1> (cited on page 10).

### [Tiller et al. 1953]

Tiller, W. A, Jackson, K. A, Rutter, J. W, and Chalmers, B (1953). “The redistribution of solute atoms during the solidification of metals”. *Acta Metallurgica*, 1 (4), pp. 428–437. URL: <http://www.sciencedirect.com/science/article/pii/0001616053901266> (cited on page 5).

### [WSA 2014]

WSA (2014). *World Steel Association: Statistics archive*. URL: <http://www.worldsteel.org/statistics/statistics-archive.html> (cited on page 10).

### [Xu et al. 1991]

Xu, D. and Li, Q. (1991). “Gravity- and Solidification-Shrinkage-Induced Liquid Flow in a Horizontally Solidified Alloy Ingot”. *Numerical Heat Transfer, Part A: Applications*, 20 (2), pp. 203–221. URL: <http://dx.doi.org/10.1080/10407789108944817> (cited on page 6).